Journal of Visualization, Vol. 11, No. 3 (2008)247-255

Regular Paper

Simultaneous Imaging Techniques for Temperature and Velocity Fields in Thermal Fluid Flows

Fujisawa, N.*, Funatani, S.* and Watanabe, Y.*

* Visualization Research Center, Niigata University, 8050 Ikarashi-2, Niigata, 950-2181, Japan. E-mail: fujisawa@eng.niigata-u.ac.jp

Received 8 November 2007
Revised 31 January 2008

Abstract : In this paper, non-intrusive imaging techniques for simultaneously measuring temperature and velocity fields of thermal liquid flows are described. The experimental methods for temperature imaging considered here are the thermo-sensitive liquid crystal tracers and the laser-induced fluorescence, which are combined with particle image velocimetry (PIV) to measure simultaneously the corresponding 2D and 3D velocity fields. The features of these experimental methods and characteristics are examined, covering the measurable temperature range, uncertainty of measurement, time response and so on. The successful examples of simultaneous measurement of temperature and velocity fields are described for turbulent Rayleigh-Bérnard convection of a horizontal fluid layer and turbulent buoyant plume issuing from a circular nozzle, and their physical mechanisms of transport phenomena are explained.

Keywords : Measurement, Visualization, Temperature, Velocity, Liquid crystal, LIF, PIV.

1. Introduction

The development of experimental methods for measuring temperature and velocity in a thermal fluid flow has been an important topic of interests to understand the transport phenomenon of heat and fluid flow in various fields of engineering. In order to study the heat and momentum transfer in the thermal fluid flow, the temperature and velocity field plays an important role in determining the physical properties in the transport phenomena. Hence, non-intrusive imaging techniques have been studied in recent years to measure the temperature and velocity field without disturbing the transport phenomena.

In the past, simultaneous imaging techniques of temperature and velocity have been studied by using the thermo-sensitive liquid-crystal tracers (TLC). This method relies on the color change of liquid-crystal tracers suspended in a fluid flow with respect to temperature variations. The color of liquid crystal changes from red at low temperatures to green, blue and violet at high temperatures, when they are illuminated by white light. This method can be extended to the simultaneous measurement of temperature and planar velocity field combining with the particle image velocimetry (PIV) (Hiller and Kowalewski, 1989; Gluckman et al., 1993; Kimura et al., 1998; Fujisawa and Funatani, 2000; Park et al., 2001; Banerjee, J. et al., 2006).

The non-intrusive temperature measurement of liquid flow is also possible using the laser-induced fluorescence (LIF). This method relies on the temperature sensitivity of the fluorescence dye induced by a laser. There were fewer studies on LIF technique in comparison with the liquid-crystal visualization technique, but it is becoming more popular in recent years due to the development of high performance imaging devices. This technique is extended to the simultaneous

measurement of temperature and velocity field in recent years in combination with PIV (Hishida and Sakakibara, 2000; Funatani et al., 2004; Reungoat et al., 2007). It is well known that the accuracy of LIF measurement is improved by the introduction of two-color LIF technique (Sakakibara and Adrian, 1999; Funatani et al., 2004; Hirasawa et al., 2007). This technique eliminates the influence of laser intensity fluctuations, which is a significant error source in the temperature measurement by the single LIF.

In the present paper, recent advances of simultaneous imaging of temperature and velocity field are described by comparing the characteristic features of thermo-sensitive liquid-crystal and laser-induced fluorescence in combination with various PIV techniques, which allow the understanding of characteristic features of these experimental methods. The successful examples of simultaneous imaging of temperature and velocity field are shown for the turbulent Rayleigh-Bérnard convection and the turbulent buoyant plume to study the characteristics of heat and fluid flows.

2. TLC and LIF for Temperature Measurement

The performance of temperature imaging by thermo-sensitive liquid-crystal tracers and laser-induced fluorescence is comparatively studied in this section to characterize these experimental methods. The items for comparison cover the characteristic features of illumination and imaging sensors, measurable temperature range, temperature uncertainty and resolution in space and time.

The experimental system for temperature imaging consists of illumination light, imaging device and the temperature-sensitive sensors. The illumination for TLC is provided by a white light source, such as xenon or metal halide lump. While, the illumination for LIF is supplied by lasers, such as Ar or Nd:YAG. Thus, the light-sheet thickness of the illumination can be made thinner for LIF than that for TLC, so that depth-wise spatial resolution is higher for LIF than TLC. The imaging device for TLC system uses a 3CCD color camera, while the LIF system needs higher intensity-resolution cameras. Note that the accuracy of temperature measurement by LIF depends highly on the intensity resolution. Thus, the experimental cost for LIF system is much expensive than that for TLC system. However, there is a limit of TLC system in the measurable temperature range due to the color characteristics of liquid crystal itself, which is known to be less than about 10 K. While, the measurable temperature range for LIF system covers the whole liquid temperature range from 0 to 100 ˚C.

The uncertainty of temperature measurement by TLC system depends mostly on the color temperature relationship, where HSI color format is often used for describing the color (H: hue, S: saturation, I: intensity). The uncertainty of color to temperature transformation is estimated as 0.27 K for the measurable temperature range of 2.3 K using the standard H calibration, but it decreases to 0.06 K using the three-parameter calibration technique in HSI (Fujisawa and Hashizume, 2001). On the other hand, the temperature uncertainty of LIF system depends on the intensity resolution. When 14 bit CCD camera is used for the LIF system, the temperature uncertainty is reported as 0.17 K in the temperature range of 20 K (Sakakibara and Adrian, 2004). The other important issue of temperature measurement is the time response of the temperature sensors, which are an order of msec for the TLC and an order of nsec for the LIF. Therefore, the TLC system is limited to slowly fluctuating thermal flows.

3. Experimental Methods

3.1 Combined TLC PIV System

The simultaneous measurement of temperature and three-components of velocity in a planar section has been measured using a combined TLC stereo PIV system, which consists of a white light illumination and two color 3CCD cameras as shown in Fig. 1. The two color CCD cameras are situated on both sides of the observation axis symmetrically to form a stereo PIV configuration. The off-axis half angle of the cameras is set to 30˚. It should be noted that the optical lens of the camera and the image plane are parallel. Thus, the present camera arrangement employs the angular

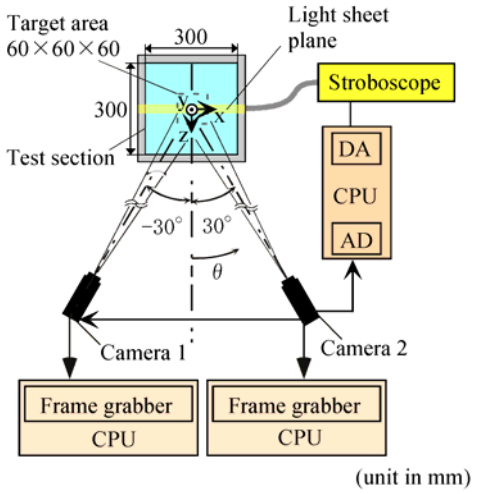

Fig. 1. Experimental setup for combined TLC stereo PIV system.

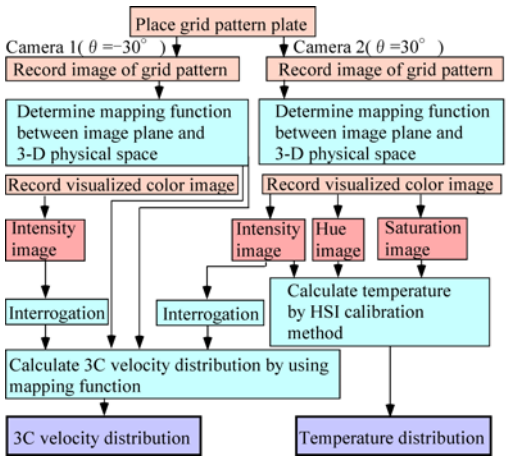

Fig. 2. Flow chart of temperature and velocity analysis.

displacement without enforcing the Scheimpflug condition. The high-intensity illumination of the light sheet was provided from a stroboscope to obtain highly focused images by this camera configuration. The color images are digitized by the frame grabber, which is installed to a personal computer. The spatial resolution of the color CCD camera is 768× 494 pixels for each RGB with 8 bits and that of the frame grabber is 640 × 480 pixels. The color of the liquid crystal changes with the observation angle variation, so that it is important to set the camera for temperature measurement to a position with highest temperature sensitivity. The experimental result shows that the temperature sensitivity is highest on the right camera in this system (Fujisawa et al., 2004). Note that the color to temperature calibration of liquid crystal tracers is carried out in a uniform temperature field. The liquid crystal tracers are chiral-nematic type having the diameter of 10 μm and the density of 1.02.

The flow chart of image analysis is displayed in Fig. 2. The analysis of color to temperature transformation is conducted pixel by pixel using a three-parameter calibration in HSI color format to minimize the calibration error of temperature (Fujisawa and Funatani, 2000). The corresponding velocity field is analyzed by cross-correlation algorithm with sub-pixel analysis. Note that the introduction of additional nylon tracers of 50 μm in diameter improves the accuracy of velocity measurement by setting the particle image size to an optimum value of about 2 pixels in the image (Fujisawa and Hashizume, 2001). The three-components of velocity field in a planar section are measured by the stereo PIV analysis using the three-dimensional calibration algorithm. For details see Funatani and Fujisawa (2002).

The combined TLC stereo PIV system has been extended to three-dimensional system by the introduction of light-sheet traversing device. By traversing two parallel light sheets normal to the measurement plane at constant velocity driven by a stepping motor, the system can measure the temperature and three-components of velocity in the three-dimensional flow field. Such system is called combined TLC scanning stereo PIV. In this system, two parallel light-sheets are provided from metal halide lumps with rotary shutter mechanism (Fujisawa et al., 2005), which allows high intensity illumination for the measurement of velocity at various planar-sections in the three-dimensional flow field. Details of the pulse illumination system are described in Fujisawa et al. (2005). It is to be noted that this illumination system provides higher intensity than that of the stroboscope due to the integrating effect of longer period of illumination. However, the application of this system is limited to thermal flows of slowly moving fluid, such as the thermal convection. This is due to the limited frame rate and the traversing speed of the light sheets.

3.2 Combined LIF PIV System

The simultaneous measurement of temperature and velocity field is carried out using a color CCD camera with an Ar laser sheet, which is shown in Fig. 3. The color filter of the camera is used to separate the two LIF images for temperature measurement and PIV images for velocity

measurement. Note that R, G, B filters of the color CCD camera transmit the light having a wavelength ranging from 575 nm to 640 nm, 490 nm to 575 nm and 400 nm to 485 nm, respectively. Illumination by Ar laser (wavelength 488 nm) is used as an excitation of Rhodamine B (emission wavelength 575 nm) and Rhodamine 110 (emission wavelength 520 nm). The nylon tracer particles of 10 μm in diameter are added to the test fluid for velocity measurement. The red filtered image and the green filtered image are used for temperature measurement with two-color LIF, and the blue filtered image is used for the velocity measurement by PIV. Although the tracer image appears weakly on the G image, such image noise is eliminated using the image processing with a median filter of 7 × 7 pixels. The temperature measurement is carried out using a calibrated relationship between R/G and temperature T, which has been obtained from uniform temperature field. The particle images captured in two sequential field images of time interval 1/60 s are analyzed by cross-correlation algorithm with sub-pixel analysis. For details see Funatani et al. (2004).

The instantaneous temperature and velocity field is also possible by two-color LIF using an illumination by Nd:YAG pulsed lasers (wavelength 532 nm, power 50 mJ), which is shown in Fig. 4. Experiments are carried out using two CCD cameras (1280× 1024 pixels with 12 bit) for temperature measurement and a CCD camera (1018× 1008 pixels with 8 bit) for planar velocity measurement (Watanabe et al., 2007). Rhodamine B (peak emission wavelength 610 nm) and the Fluorescein Sodium (peak emission wavelength 545 nm) are used as temperature sensitive dyes. The fluorescent lights are separated by the dichroic mirror, which reflects the light having wavelength shorter than 570 nm and transmits the light having wavelength longer than 570 nm. In order to remove the influence of incident laser light on the image of Fluorescent Sodium, a notch filter is placed to remove the laser light at the wavelength 532 nm. Note that the CCD camera with frame straddling function is placed on the other side of the test section to measure the velocity field by PIV, so that this system is applicable to high-speed flows.

4. Results and Discussion

4.1 Combined TLC PIV for Application to Rayleigh Bérnard Convection

The combined TLC stereo PIV system is applied to the simultaneous measurement of temperature and velocity in a horizontal fluid layer of water in Rayleigh-Bénard convection at Rayleigh number Ra $(=\beta\, g\, \Delta T\, h^3/\nu\, \kappa)=2.9 \times 10^7$ (β = thermal expansion coefficient, g = gravitational acceleration, ΔT = temperature difference between upper and lower surfaces, h = height of fluid layer, κ = thermal diffusivity, ν = kinematic viscosity). Note that the height of the fluid layer is 60mm and the temperatures of the bottom and top surface are kept constant at 28.5 ˚C and 33.5 ˚C, respectively.

Figures 5(a) and (b) show a typical example of temperature and velocity distributions across the fluid layer of Rayleigh-Bénard convection. The temperatures are expressed by isothermal

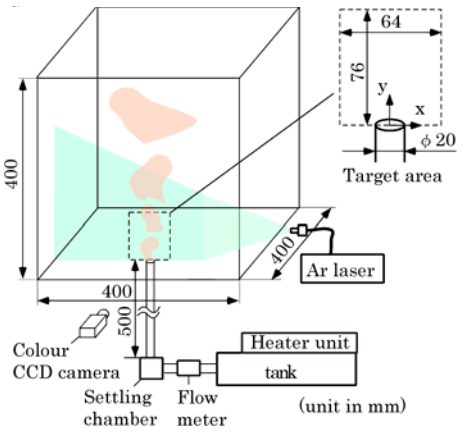

Fig. 3. Experimental setup for buoyant plume.

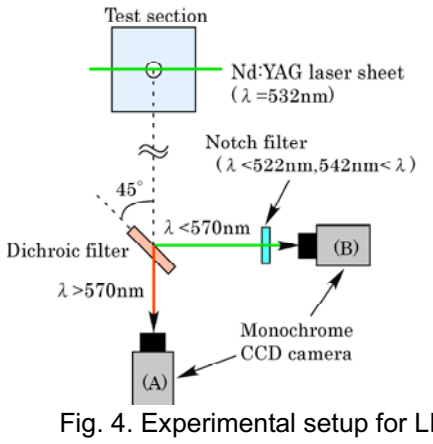

Fig. 4. Experimental setup for LIF.

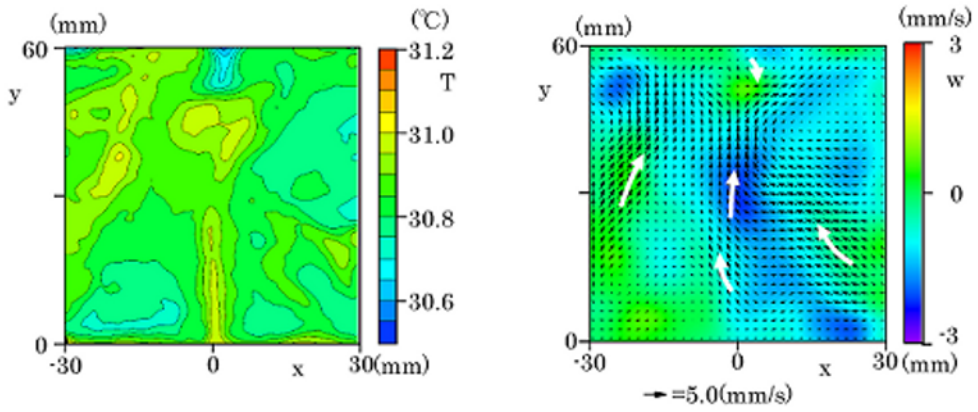

(a) (b)

Fig. 5. Temperature and velocity contours of Rayleigh Bérnard convection, (a) Temperature distribution, (b)Velocity distribution.

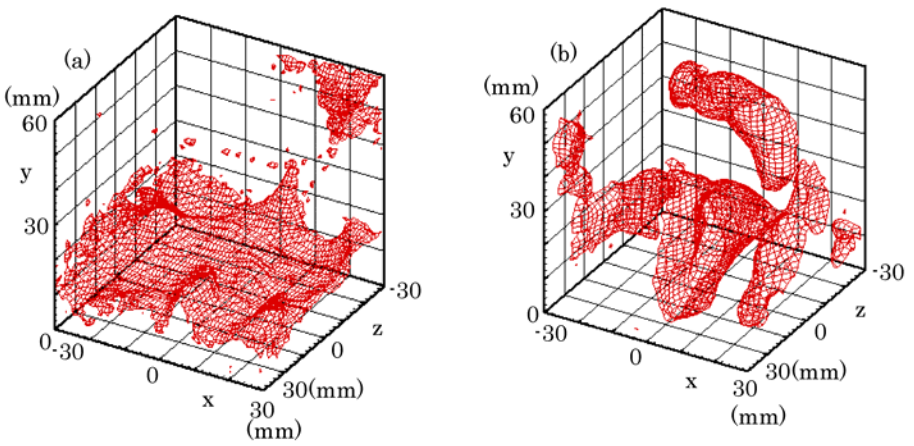

Fig. 6. Three-dimensional contours of temperature and velocity fields, (a) Temperature, (b) Velocity.

contour-lines, covering the vertical observation area of 60 mm × 60 mm. The top and bottom boundaries correspond to the cold and hot boundaries, respectively. The measured temperature contours (Fig. 5(a)) show that the high temperature area is generated from the bottom boundary and grows upward, which corresponds to the generation of hot plume from the heated boundary. On the contrary, the cold plume moves down from the top boundary. The corresponding velocity field (Fig. 5 (b)) shows the behavior of three velocity components in the fluid layer. The magnitude of out-of-plane velocity w is displayed by the color bar. It is seen that the velocity magnitude near the top and bottom boundaries is small reflecting the wall damping effect of the velocity field near the wall. On the contrary, the velocity magnitude in the middle of the fluid layer increases by the growth of hot plumes from the bottom boundary. It is found that the area of large vertical-velocity in the middle of the fluid layer meets the position of high temperature area of the hot plume, so that the vertical velocity is originated from hot plumes. On the other hand, the downward movement of the cold plume is observed near the top boundary. Thus, the structure of the velocity field in the Rayleigh-Bénard convection is highly three-dimensional due to the interaction of hot and cold plumes.

The simultaneous measurement of temperature and velocity in three-dimensional flow field of turbulent Rayleigh-Bérnard convection is carried out using the scanning TLC stereo PIV system. Figure 6(a) shows the isothermal contour surfaces of temperature at T= 28.6 ˚C. The result indicates the presence of hot plume generated from the high temperature region near the lower boundary. The three-dimensional contour maps of the constant vertical velocity are shown in Fig. 6(b), which

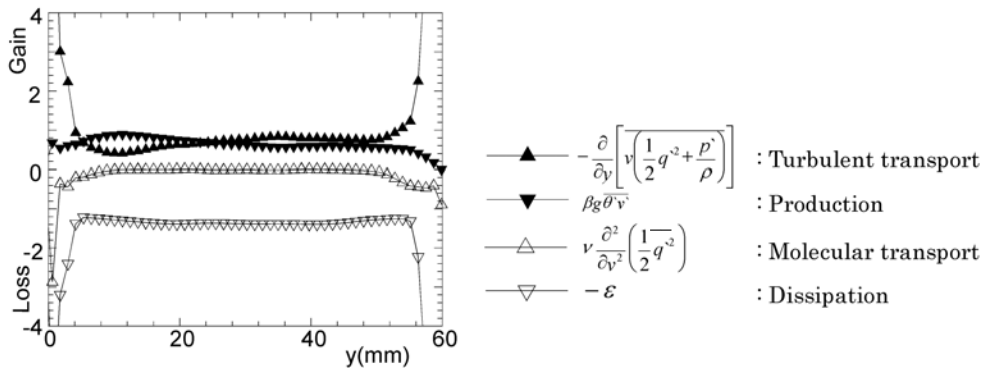

Fig. 7. Turbulence energy balance.

corresponds to upward velocity v = 1.1 mm/s. These velocity contours shares common features to those of the temperature contour in Fig. 6(a). However, the deviation of the velocity contour from the temperature contour is clearly observed in the middle of the fluid layer. Thus, the result indicates that the correlation of velocity and temperature field observed near the upper and lower boundaries is weakened with an increase in the distance from the boundaries, which is due to the growth of turbulent mixing in the middle of the fluid layer.

The combined TLC planar PIV is applied to the measurement of turbulence energy balance in the vertical cross-section of the Rayleigh Bérnard convection, which is shown in Fig. 7.

The turbulence energy equation is written as follows;

$$-\frac{\partial}{\partial y}\left[\overline{v\left(\frac{1}{2}q'^2+\frac{p'}{\rho}\right)}\right]+\beta g\overline{t'v'}-\nu\frac{\partial^2}{\partial y^2}\left(\frac{1}{2}\overline{q'^2}\right)-\varepsilon=0 \quad (1)$$

The first term on the left-hand-side denotes the turbulent transport of turbulence energy q'^2, the second term is the buoyant production, the third term is the molecular transport, and the fourth term is the viscous dissipation. p': pressure fluctuation, t': temperature fluctuation, v': vertical velocity fluctuation. Note that the turbulent transport is evaluated from the residual using the experimental data and this equation, because it involves the pressure fluctuation term, which is difficult to measure. The evaluation of each term of this equation is carried out using 1,000 pair images taken at every 10 second (Hashizume et al., 2006). The experimental result shows that the production and the turbulent transport terms balance the dissipation term in the convection layer. While, the magnitude of turbulent transport and the dissipation increase rapidly as the wall boundaries are approached. Thus, the turbulence energy is generated almost uniformly in the convection layer and is transferred to the near-wall region to dissipate the energy. These experimental results indicate that the large magnitude of turbulence energy is transported across the fluid layer and is dissipated in the wall layers, which suggests an importance of the wall layer for sustaining the turbulence energy balance in the Rayleigh-Bénard convection.

4.2 Combined LIF PIV System for Application to Buoyant Plume

The simultaneous measurement of temperature and velocity by two-color LIF PIV using Ar laser is applied to the turbulent buoyant plume issuing from a circular nozzle in a stagnant surrounding of cold water, where the source Froude number is $Fr_0(= V_0/\sqrt{(\rho_c-\rho_h)dg/\rho_h})$= 0.20 and the Reynolds number is $Re(= V_0 d/\nu)$= 420, where d: nozzle diameter (= 20 mm), g: gravitational acceleration, V_0: nozzle exit velocity (= 10 mm/s), ν: kinematic viscosity of hot water, ρ: density of fluid, and subscripts c and h denote cold and hot state, respectively. The hot and cold water are supplied from the heating units with thermal controller. The temperatures of the hot water and the cold water are 60 deg and 30 deg, respectively.

The statistical properties of the buoyant plume in the initial region are evaluated from 1,000 instantaneous temperature and velocity field, which are taken at every 1 second. The contours of

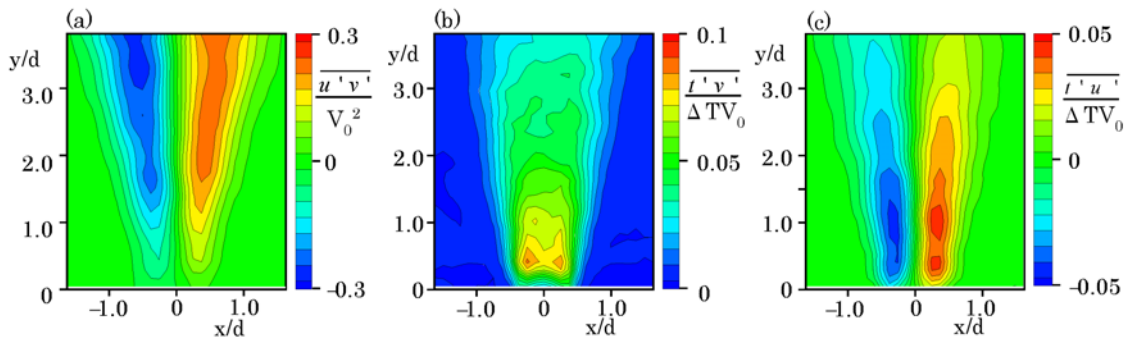

Fig. 8. Statistical properties of buoyant plume, (a) Reynolds stress, (b) Vertical turbulent heat flux, (c) Horizontal turbulent heat flux.

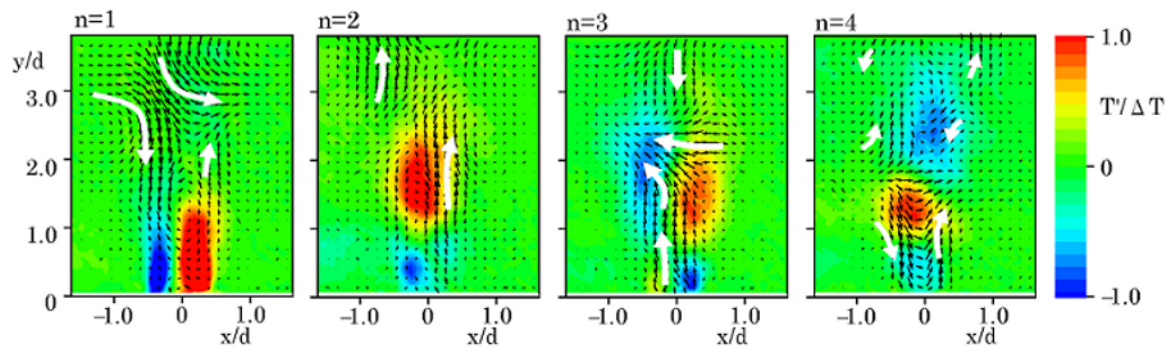

Fig. 9. Eigenfunctions of temperature and velocity field.

Reynolds stress $\overline{u'v'}/V_0^2$ and vertical and horizontal turbulent heat fluxes $\overline{t'v'}/\Delta TV_0, \overline{t'u'}/\Delta TV_0$ in the buoyant plume are given in Figs. 8(a), (b) and (c), respectively. The Reynolds-stress distribution indicates the change of sign at the plume centerline, and the magnitude of Reynolds stress increases gradually with the distance from the nozzle exit. The contour of vertical turbulent heat flux shows local peaks near the nozzle exit and it decreases gradually with an increase in the distance from the nozzle, while the contour of horizontal turbulent heat flux changes the sign at the plume centerline, which is similar to the Reynolds stress contour. It should be mentioned that the flow properties observed far from the nozzle approach those of the fully developed buoyant plume measured by point-wise techniques (Murota et al., 1989; Shabbir and George, 1994), which suggests the validity of the present field measurement using combined two-color LIF PIV.

In order to examine the structure of turbulent plume statistically, the snapshot proper orthogonal decomposition (POD) (Breuer and Sirovich, 1991; Berkooz et al., 1993) is introduced into the analysis of experimental data measured by the two-color LIF PIV illuminated by Nd:YAG pulsed lasers. The experimental conditions are the same as the LIF PIV measurement with Ar laser in the previous paragraph. The POD analysis is performed over the number of data 600, which corresponds to total observation time of 10 minutes. Figure 9 shows eigenfunctions of temperature and velocity fluctuation at the first 4 modes. At the lowest mode n = 1, a large magnitude of temperature fluctuations with positive and negative sign appears near the nozzle exit. Thus, the temperature eigenfunction shows the asymmetrical shape with respect to the plume centerline. With an increase in mode number n, the temperature eigenfunction is still asymmetrical, but the magnitude of the eigenfunction is reduced and the scale of the structure becomes small. Note that the decrease in temperature eigenfunction corresponds to the reduction in the energy of temperature fluctuations. On the other hand, the eigenfunctions of velocity fluctuation shows large downward velocity on the left hand side of the plume and small upward velocity on the right hand side at n = 1. The clockwise vortices are formed on the left-hand side of the plume and on the lower right hand side of the plume. The counter clockwise vortex is found on the upper right hand side of the plume. Thus, the velocity eigenfunction shows an asymmetrical contour with respect to the plume centerline. Note that the scale of the velocity eigenfunction decreases with an increase in mode number, which is similar to

that of the temperature eigenfunction. These results indicate that the temperature and velocity fields behave asymmetrically in the plume, and their fine structures are deviated from each other.

5. Conclusions

The experimental techniques for imaging simultaneously the temperature and the velocity field of thermal liquid flows are described using liquid crystal tracers and laser-induced fluorescence, in combination with various types of PIV techniques. The former method is capable to measure the thermal flow in relatively small temperature range with a low cost, and the latter method is applicable to that of relatively large temperature range with reasonable accuracy. These experimental methods are applied to the simultaneous imaging of temperature and velocity field of turbulent Rayleigh-Bérnard convection and turbulent buoyant plumes, and the transport phenomena of heat and fluid-flow are explained by the experimental data.

Acknowledgments

This work was supported by grant-in aid of Japanese Ministry of Education, Science and Culture (nos. 12650158, 16560139). The authors would like to acknowledge cooperation and suggestion by Prof. RJ Adrian of Arizona State University and Dr. Y. Hashizume of former post-doc fellow at Niigata University.

References

Banerjee, J., Bharadwaj, R. and Muralidhar, K., Experimental Study of Convection in a Model Czochralski Crucible Using Liquid Crystal Thermography, Journal of Visualization, 9-1 (2006), 111-119.

Berkooz, G., Holmes, P. and Lumley, J. L., The Proper Orthogonal Decomposition in the Analysis of Turbulent Flows, Annual Review of Fluid Mechanics, 25 (1993), 539-575.

Breuer, K. and Sirovich, L., The Use of the Karhunen-Loeve Procedure for the Calculation of Linear Eigenfunctions, Journal of Computational Physics, 96 (1991), 277-296.

Fujisawa, N., Adrian, R. J., Three-dimensional Temperature Measurement in Turbulent Thermal Convection by Extended Range Scanning Liquid Crystal Thermometry, Journal of Visualization, 1-4 (1999), 355-364.

Fujisawa, N. and Funatani, S., Simultaneous Measurement of Temperature and Velocity in a Turbulent Thermal Convection by the Extended Range Scanning Liquid Crystal Visualization Technique, Experiments in Fluids, 29 (2000), s158-165.

Fujisawa, N., Funatani, S. and Katoh, N., Scanning Liquid-crystal Thermometry and Stereo Velocimetry for Simultaneous Three-dimensional Measurement of Temperature and Velocity Field in a Turbulent Rayleigh-Bérnard Convection, Experiments in Fluids, 38 (2005), 291-303.

Fujisawa, N. and Hashizume, Y., An Uncertainty Analysis of Temperature and Velocity Measured by a Liquid Crystal Visualization Technique, Measurement Science and Technology, 12 (2001), 1235-1242.

Fujisawa, N., Nakajima, T., Katoh, N. and Hashizume, Y., An Uncertainty Aanalysis of Temperature and Velocity Measured by Stereo Liquid-crystal Thermometry and Velocimetry, Measurement Science and Technology, 15 (2004), 799-806.

Funatani, S. and Fujisawa, N., Simultaneous Measurement of Temperature and Three Velocity Components in Planar Cross Section by Liquid-crystal Thermometry Combined with Stereoscopic Particle Image Velocimetry, Measurement Science and Technology, 13 (2002), 1197-1205.

Funatani, S., Fujisawa, N. and Ikeda, H., Simultaneous Measurement of Temperature and Velocity Using Two-color LIF Combined with PIV with a Color CCD Camera and Its Application to the Turbulent Buoyant Plume," Measurement Science and Technology, 15 (2004), 983-990.

Gluckman, B.J., Willaime, H. and Gollub. J.P., Geometry of Isothermal and Isoconcentration Surfaces in Thermal Turbulence, Physics of Fluids, A5 (1993), 647-661.

Hashizume, Y., Watanabe, M. and Fujisawa, N., Measurement of Turbulence Energy Balance in Rayleigh-Bérnard Convection by Liquid Crystal Thermometry and Velocimetry, Journal of the Visualization Society of Japan, 26,Suppl 1(2006), 111-114 (in Japanese).

Hiller, W. J. and Kowalewski, T. A., Simultaneous Measurement of Temperature and Velocity Fields in Thermal Convective Flows, Flow Visualization, Vol.4(ed Varet, C.), (1987), 617-622, Hemisphere, Washington.

Hirasawa, T., Kaneba, T., Kamata, Y., Muraoka, K. and Nakamura, Y., Temperature Dependence of Intensities of Laser-Induced Fluorescences of Ethylbenzene and Naphthalene Seeded in Gas Flow at Atmospheric Pressure; Implications for Quantitative Visualization of Gas Temperature, Journal of Visualization, 10-2(2007), 197-206.

Kimura, I., Hyodo, T. and Ozawa, M., Temperature and Velocity Measurement of a 3-D Thermal Flow Field Using Thermo-sensitive Liquid Crystals, Journal of Visualization, 1-2 (1998), 145-152.

Hishida, K. and Sakakibara, J., Combined Planar Laser-induced Fluorescence: Particle Image Velocimetry Technique for Velocity and Temperature Fields, Experiments in Fluids, 29 (2000), s129-140.

Murota, A., Nakatsuji, K. and Tamai, M., Experimental Study on Turbulence Structure in Turbulent Plane Forced Plume, Journal of Japan Society of Civil Engineering, 405 (1989), 79-87 (in Japanese).

Park, H.G., Dabiri, D. and Gharib, M., Digital Particle Image Velocimetry/Thermometry and Application to the Wake of a Heated Circular Cylinder, Experiments in Fluids, 30 (2001), 327-338.

Reungoat, D., Riviere, N. and Faure, J.P., 3C PIV and PLIF Measurement in Turbulent Mixing; Round Jet Impingement, Journal of Visualization, 10-1 (2007), 99-110.

Sakakibara, J. and Adrian, R. J., Whole Field Measurement of Temperature in Water Using Two-color Laser Induced Fluorescence, Experiments in Fluids, 26 (1999), 7-15.
Sakakibara, J. and Adrian, R. J., Measurement of Temperature Field of a Rayleigh-Benard Convection Using Two-color Laser-induced Fluorescence, Experiments in Fluids, 37 (2004), 331-340.
Shabbir, A. and George, W. K., Experiments on a Round Turbulent Buoyant Plume, Journal of Fluid Mechanics, 275 (1994), 1-32.
Watanabe, Y., Hashizume, Y. and Fujisawa, N., Temperature Measurement by Two-Color LIF Technique Using Nd:YAG lasers, Journal of Visualization, 10-4 (2007), 343-344.

Author Profile

Nobuyuki Fujisawa: After graduating from Tohoku University (Dr E. 1983), he joined Gunma University and worked as an associate professor since 1991. He has been a professor of Niigata University since 1997, and now he is a director of Visualization Research Center at Niigata University. His current research interests are flow visualization, non-intrusive measurement of temperature and velocity in thermal and combusting flow, and mass transport phenomena of flow accelerated erosion and corrosion problems.

Shumpei Funatani: He graduated from Graduate School of Niigata University (Dr E. 2005). He has been working at R&D department of Corona Corporation since 2004. His current research interests are flow visualization and measurement of thermal and combusting flows, development of low emission combustor using catalytic combustion and multi-fuel combustor of fuel-cell system.

Yoshie Watanabe: She graduated from Graduate School of Niigata University (Mr E. 2007). She has been working at R&D department of Thermos Corporation since 2007.